ATTITUDE DETERMINATION BY KALMAN FILTERING

James L. Farrell

Third Quarterly Progress Report

Contract NAS 5-9195

Westinghouse Electric Corporation

Aerospace Division

February, 1966

This report summarizes the work performed in the areas of analytical formulation, literature research, and digital simulation through the third quarter of Contract NAS 5-9195. The first two items are complete; the formulation is presented in the accompanying APPENDIX, which is intended for use also in the final report.

The digital program defined in the Second Quarterly Progress Report, appropriately modified and extended, has successfully been tested on the GSFC Moonlight system. Run trials have thus far been restricted to simplified cases; general system simulation and data evaluation will constitute the major task for the final quarter.

APPENDIX

This section contains the entire mathematical background for all dynamic, geometric, and statistical analyses and transformations employed in this study. Much of the theory is well established by a long history of documentation; some was taken from recent contributions to the open literature; and certain portions (specifically, the closed form rotational state transition matrix) have not, to the best of the writer's knowledge, appeared previously.

The first three appendices contain straightforward means of describing general angular motion, and Appendix D gives a well known special case solution to the rotational equations of motion. Appendix E illustrates the precession of angular momentum due to solar and gravity gradient torques, as described separately in two recent articles in the applicable literature. Appendix F discusses some recent literature regarding gravity gradient libration, and provides a restrictive closed form solution for vertically oriented satellites. The next two appendices adapt the state variable formulation to rotational systems, in preparation for the Kalman filtering operations described in Appendix I. The last two appendices illustrate the types of measurements under consideration and their allowable ranges of variation.

List of Major Notation*

Symbol	Definition
A_v	Effective vehicle area
$\underline{\underline{A}}$	Matrix of coefficients in differential equation for $\underline{\underline{\Phi}}$
a_{ij}	ij element of $\underline{\underline{A}}$

*Units for angles and their derivatives are radians and seconds.

Symbol	Definition
$\underline{\underline{B}}$	Transformation from vehicle to fixed inertial coordinates.
$\underline{\underline{B}}_n$	nth column of $\underline{\underline{B}}$
$\underline{\underline{C}}$	Transformation from vehicle to local vertical coordinates.
c_{ij}	ij element of $\underline{\underline{C}}$
$\underline{\underline{D}}$	Transformation from local vertical to fixed inertial coordinates
$\underline{\underline{G}}$	Transformation from vehicle to temporary inertial coordinates.
$\underline{\underline{G}}_n$	nth column of $\underline{\underline{G}}$
g_{ij}	ij element of $\underline{\underline{G}}$
$\underline{H}$	1 x 6 row vector of partial derivatives $\partial Y/\partial \underline{X}$
$\underline{\mathcal{H}}$	1 x 3 row vector $\left[H_1\ H_2\ H_3\right]$
$\underline{h}$	Angular momentum vector
$\underline{\underline{I}}_{nn}$	n x n identity matrix
$\underline{I}$	Unit vector along fixed inertial x-axis
$\underline{I}'$	Unit vector along temporary inertial x-axis
$\underline{i}$	Unit vector along vehicle roll axis
I	Moment of inertia (Kg - meter^2)
i	Orbital inclination angle
$\underline{J}$	Unit vector along fixed inertial y-axis
$\underline{J}'$	Unit vector along temporary inertial y-axis
$\underline{J}_v$	Unit vector along orbit pole
$\underline{j}$	Unit vector along vehicle pitch axis
$\underline{K}$	Unit vector along fixed inertial z-axis
$\underline{K}'$	Unit vector along temporary inertial z-axis

Symbol	Definition
$\underline{K}_V$	Unit vector along upward local vertical
$\underline{k}$	Unit vector along vehicle yaw axis
$\underline{K}_\beta$	Unit vector pointing to north magnetic pole of earth (fixed inertial coordinates)
$\underline{L}_1$	Unit vector normal to face of sun sensor in vehicle (vehicle coordinates)
$\underline{L}$	$\underline{U} \times \underline{L}_1$ (vehicle coordinates)
$\underline{m}$	Earth dipole moment (amp-meter^2; fixed inertial coordinates)
$\underline{N}$	Sensitivity vector in the plane of $\underline{L}$ and $\underline{U}$ (vehicle coordinates)
n_o	Orbital rate
$\underline{\underline{O}}_{mn}$	m x n null matrix (subscripts omitted for m = n = 1)
P_ρ	Solar pressure (newt. per meter^2)
$\underline{\underline{P}}$	Uncertainty covariance matrix
$\underline{Q}$	Vector from center of pressure to center of gravity in vehicle (meters; vehicle coordinates)
q	Magnitude of $\underline{Q}$
q_n	nth component of $\underline{Q}$
$\underline{R}$	Vehicle position vector w.r.t. central force field (meters; fixed inertial coordinates)
r	Magnitude of $\underline{R}$
r_1, r_2	Coupled yaw-roll libration frequencies
$\underline{S}$	Unit vector toward sunline (fixed inertial coordinates)
$\underline{S}'$	Unit vector toward sunline (temporary inertial coordinates)
$\underline{S}''$	Unit vector toward sunline (vehicle coordinates)
t	time

$\underline{U}$	Unit vector along sun sensor slit (vehicle coordinates)
$\underline{V}$	Unit vector along ($\underline{S}''$ x $\underline{U}$) (Vehicle coordinates)
$\underline{W}$	Recursive optimum linear estimator
X_1, X_2, X_3	Position state variables (Euler angles)
X_4, X_5, X_6	Velocity state variables (roll, pitch, yaw rates)
$\underline{X}$	6 x 1 state vector
$\underline{x}$	Variation of $\underline{X}$ from reference value
Y	Observable
y	Variation of Y from reference value
Z_{ij}	Coupled yaw-roll libration amplitudes
γ_n	Initial value of (n^{th}) angular displacement from local reference
$\alpha, \alpha_{hv}, \alpha_{kv}$	Angles between reference vectors for rotation analysis of symmetrical satellite
$\underline{\beta}$	Earth dipole magnetic flux density (webers/meter^2 ; fixed inertial coordinates)
$\underline{\beta}'$	Earth dipole magnetic flux density (temporary inertial coordinates)
$\underline{\beta}''$	Earth dipole magnetic flux density (vehicle coordinates)
β_n	nth component of $\underline{\beta}$
$\underline{\underline{\Gamma}}$	Transformation from local vertical to temporary inertial coordinates
$\underline{\Gamma}_n$	nth column of $\underline{\underline{\Gamma}}$
δ	Variation
$\delta_1, \delta_2, \delta_3$	Roll, pitch, and yaw libration angles
ζ	Angle between $\underline{S}''$ and $\underline{U}$
$\underline{\underline{\eta}}$	Time-varying orientation matrix for torque-free symmetrical satellite

θ	True anomaly
λ	Vehicular elevation angle
μ	Gravitational constant of central force field ($meter^3/sec^2$)
μ_β	$4\pi \times 10^{-7}$ henry/meter
ν	Dynamic coefficient ($/sec^2$)
$\digamma$	Dynamic coefficient (dimensionless)
ρ	Force due to solar pressure (newtons)
σ	Standard deviation (general)
$\underline{\underline{\Phi}}$	State transition matrix
Φ_{ij}	ij element of $\underline{\underline{\Phi}}$
Ψ_{ij}	Coupled yaw-roll libration phase angles
Ψ	Vehicular azimuth angle
Ω	Longitude of ascending node
ω_A, ω_B	Spin and precession rates for torque free symmetrical satellite
ω_n	nth component of vehicle angular rate vector (n=1,2,3)
ω_o	Argument of perigee of vehicle orbit
ω_P	Precession rate
ω_S	Sidereal rate

Subscripts

1,2,3	Pertaining to x,y, and z axes, respectively
x,y,z	Pertaining to x,y, and z axes, respectively
m	At time of mth observation
o	Orbital, initial
s	pertaining to sun
$\underline{\quad}$	vector
$\underline{\underline{\quad}}$	matrix

Superscripts	Definition
$\hat{(\ )}$	Observed or apparent value
$\tilde{(\ )}$	Error in observed or apparent value
(+)	Immediately after an observation
(-)	Immediately before an observation
$(\ )^T$	Transpose
$(\ )'$	Pertaining to temporary inertial coordinates
$(\ )''$	Pertaining to vehicle coordinates
Υ	Vernal Equinox
$[\gamma]_u$	Orthogonal transformation matrix corresponding to a positive rotation of (γ) radians about the u-axis.

APPENDIX A

CO-ORDINATE REFERENCES

As explained in the INTRODUCTION, the need for an inertial attitude reference has prompted the use of the familiar celestial sphere. For earth satellites the earth is considered as the center of the celestial sphere, but it is permissible to have the sun at the center for solar orbiters.[A-1] In either case the reference radii have fixed directions in inertial space, since (as previously discussed) the entire analysis can be conducted on the basis of a somewhat idealized astronomical geometry. Specific analytical interpretations of the celestial sphere for earth satellites and solar orbiters are described separately as follows:

Earth satellites. Figure illustrates a co-ordinate frame having an inertially fixed orientation (right hand set defined in terms of the vernal equinox and the north geodetic pole as shown) and a local vertical frame (right hand set defined in terms of the orbit pole and the instantaneous upward local vertical), with the orthogonal transformation $\underline{\underline{D}}$ between these frames defined by the commonly designated angles.[A-2] Since the solar "orbit" is characterized by zero nodal longitude and an ecliptic inclination angle (i_s), the unit sunline vector in fixed inertial coordinates is

$$\underline{S} = \begin{bmatrix} \cos\theta_s \\ \cos i_s \sin\theta_s \\ \sin i_s \sin\theta_s \end{bmatrix} \qquad (A\text{-}1)$$

where (θ_s) is determined by the time of the year past March 21.

Solar orbiters. With the sun at the center of the celestial sphere, Fig. is re-interpreted to account for the following modifications:

(1) The sunline in vehicle co-ordinates is along the downward local vertical.

INERTIAL REFERENCE

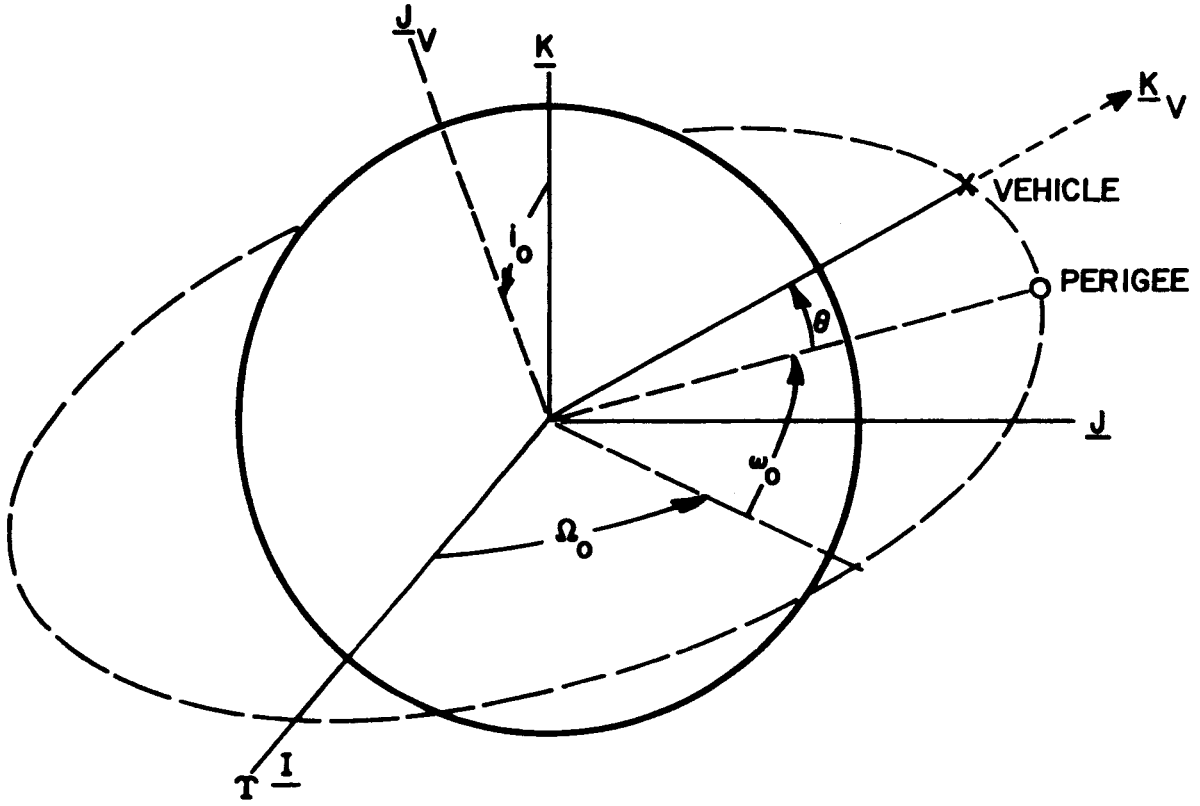

$$\underline{\underline{D}} \triangleq \left[-\Omega_o\right]_Z \left[-i_o\right]_X \left[-(\omega_o + \theta)\right]_Z \begin{bmatrix} 0 & 0 & 1 \\ 1 & 0 & 0 \\ 0 & 1 & 0 \end{bmatrix}$$

SUNLINE

$$\underline{S} = \left[-i_s\right]_X \left[-\theta_s\right]_Z \begin{bmatrix} 1 \\ 0 \\ 0 \end{bmatrix}$$

VEHICLE

$$\begin{bmatrix} \underline{I} \\ \underline{J} \\ \underline{K} \end{bmatrix} = \underline{\underline{D}} \begin{bmatrix} \underline{I}_V \\ \underline{J}_V \\ \underline{K}_V \end{bmatrix}$$

(2) The reference line for the true anomaly (θ) is the perihelion.

(3) The fixed inertial z-axis is the pole of the ecliptic. The orbital inclination (i_o) is reinterpreted accordingly.

With the above definitions it is now possible to present the remaining attitude formulations, which are uniformly applicable to earth and sun orbiters. If the transformations from vehicle axes to fixed inertial and to local vertical coordinates may be designated as B and C, respectively, it follows that

$$\underline{\underline{B}} = \underline{\underline{D}}\,\underline{\underline{C}} \qquad (A\text{-}2)$$

Since the attitude determination procedure involves a formulation in terms of nonredundant parameters (i.e., state variables), we are interested ultimately in a set of Euler angles* rather than the direction cosines themselves. Theoretically there is great flexibility in the choice of Euler angle arrangements and sequences, but the overall transformation must be defined such that the well-known singularity problem will be avoided. A convenient nonsingular definition of the transformation is derived as follows:

During the "present" interval (i.e., $t_{m-1} < t < t_m$) the true vehicle attitude relative to its true previous (t_{m-1}) orientation is given by

$$\underline{\underline{G}} = \underline{\underline{B}}_{m-1}^{T}\,\underline{\underline{B}} \qquad (A\text{-}3)$$

Combined with equation (A-2) and the definition of the known, independently time-varying matrix $\underline{\underline{D}}$ (Fig.), it follows that

$$\underline{\underline{G}} = \underline{\underline{\Gamma}}\,\underline{\underline{C}} \qquad (A\text{-}4)$$

where $\underline{\underline{\Gamma}}$ is the time-varying matrix defined in figure . It can thus be seen that Euler's equations of motion (which, to look ahead for a moment, contain torques that vary as a function of $\underline{\underline{B}}$ and $\underline{\underline{C}}$) can be written in terms of $\underline{\underline{G}}$ and other transformations which depend only upon the current translational

*Although there are other three-parameter sets of attitude variables, [A-3] there are no all-attitude three-parameter sets without singularities or discontinuities. It follows that Euler angles represent as suitable a parameter set as any other known formulation.

SHIFTING INERTIAL REFERENCE

AT TIME t_{m-1} , $\underline{\underline{B}}_{m-1} = \underline{\underline{D}}_{m-1}\,\underline{\underline{C}}_{m-1}$

AT TIME t , $\underline{\underline{B}} = \underline{\underline{D}}\,\underline{\underline{C}}$

TRANSFORMATION TO TEMPORARY REFERENCE:

$$\underline{\underline{G}} \triangleq \underline{\underline{B}}^T_{m-1}\,\underline{\underline{B}} = \underline{\underline{\Gamma}}\,\underline{\underline{C}};$$

$$\underline{\underline{\Gamma}} \triangleq \underline{\underline{C}}^T_{m-1}\,\underline{\underline{D}}^T_{m-1}\,\underline{\underline{D}} = \underline{\underline{C}}^T_{m-1}\begin{bmatrix}0&1&0\\0&0&1\\1&0&0\end{bmatrix}\left[\theta_{m-1}-\theta\right]_Z\begin{bmatrix}0&0&1\\1&0&0\\0&1&0\end{bmatrix}$$

EQUATIONS OF MOTION

EULER'S EQUATIONS:

$$I_n\dot{\omega}_n + (I_{n+2}-I_{n+1})\omega_{n+2}\omega_{n+1} = 3(\mu/r^3)\,c_{3,n+2}c_{3,n+1}(I_{n+2}-I_{n+1}) + \rho\left[\underline{Q}\times\underline{\underline{B}}^T\underline{S}\right]_n$$

EQUIVALENCES:

$$c_{ij} = \underline{\Gamma}_i^T\,\underline{G}_j$$

$$\left[\underline{Q}\times\underline{B}^T\underline{S}\right]_n = q_{i+1}\,\underline{G}^T_{i+2}\underline{S}' - q_{i+2}\,\underline{G}^T_{i+1}\underline{S}'$$

$$\xi_n \triangleq (I_{n+2}-I_{n+1})/I_n$$

$$\nu_{ij} = \rho q_i / I_j$$

STATE VARIABLE FORM:

$$\dot{\omega}_n = \xi_n(-\omega_{n+1}\,\omega_{n+2} + 3\mu\,\underline{\Gamma}_3^T\,\underline{G}_{n+2}\,\underline{\Gamma}_3^T\,\underline{G}_{n+1}/r^3) + \nu_{n+1,n}\,\underline{G}^T_{n+2}\,\underline{S}'$$

$$-\nu_{n+2,n}\,\underline{G}^T_{n+1}\,\underline{S}' \quad ; n = 1, 2, 3$$

motion and the rotational motion which occurred prior to the interval under consideration. Since these other transformations ($\underline{\underline{B}}_{m-1}$, $\underline{\underline{C}}_{m-1}$, $\underline{\underline{\Gamma}}$) are obviously known during the present interval, the torques in Euler's equations can be considered as known functions of $\underline{\underline{G}}$. This matrix, in turn, can be written as a sequence of roll, pitch, and yaw turns;

$$\underline{\underline{G}} = \left[X_3\right]_z \left[X_2\right]_y \left[X_1\right]_x \qquad \text{(A-5)}$$

For non-spinning satellites these angles cannot grow to large values (in particular, X_2 cannot grow near $\pi/2$) during any reasonable measurement interval. For spinning satellites, the arbitrary nomenclature of the three vehicle axes can easily be chosen w.r.t. the initial $\underline{\underline{C}}$ - matrix such that, for a given initial vehicle angular rate and a given dynamical environment, the angle (X_2) could not grow near $\pi/2$ during a specified measurement interval. This convention therefore maintains a well-defined set of Euler angles.

A nonsingular three-parameter set of attitude variables can therefore be obtained by using a temporary inertial reference, which is repeatedly shifted to the orientation corresponding to the time of the most recent measurement. With this formulation, the rotational equations of motion can be written with forcing functions (torques) which vary as known functions of well-defined Euler angles (X_1, X_2, and X_3). Attention will now be drawn to the form of these forcing functions and the resulting form of the dynamical equations.

APPENDIX B

EULER'S DYNAMIC EQUATIONS

The present investigation is aimed primarily at establishing the feasibility of minimum variance attitude determination, rather than a rigorously precise simulation involving complete characterization of all higher order errors and anomalies. In the interest of obtaining a computer program with a minimum of time-consuming numerical integration routines, the analytical model idealized to some extent wherever the simplifications do not affect the magnitude of the torques to be encountered.

An orbiting satellite with a non-spherical inertia ellipsoid experiences a well known torque due to gravity gradient. It can be shown that, for an ideal inverse square law gravitational field, this torque is*

$$\underline{T}_g = (3\mu/r^3) \begin{bmatrix} c_{33}\, c_{32}\, (I_3 - I_2) \\ c_{31}\, c_{33}\, (I_1 - I_3) \\ c_{32}\, c_{31}\, (I_2 - I_1) \end{bmatrix} \qquad \text{(B-1)}$$

As a simple illustration of this expression consider a satellite with z-axis symmetry (so that $I_2 = I_1$) and with $I_3 < I_1$. When the vehicle is nearly aligned with local axes the small angle transformation matrix $\underline{\underline{C}}$ has nearly skew-symmetric off-diagonal elements. If $\underline{k}$ has a positive projection on the $\underline{J}_v$ axis, then (c_{23}) is positive; (c_{32}) is therefore negative, and T_{g1} is positive, essentially proportional to (c_{23}). This tends to align $\underline{k}$ with the local vertical axis $\underline{K}_v$.

*Actually it is shown in reference B-1 that small gravity gradient torques can be present even when the three principal moments of inertia are equal. Another complication arising from non-ideal geometry is the change in torque due to a non-uniform gravity field. Gravity gradient torques with an oblate earth are analyzed in reference B-2.

In addition to the above torque due to gravity gradient, there is a torque due to solar pressure when the vehicle cg does not coincide with its center of pressure. Assuming specular reflection from a homogeneous spherical surface, the appropriate force (ρ) is the product of the effective vehicle area (A_v) multiplied by the solar pressure (0.9 newton per square meter at 1.0 AU, and inversely proportional to the square of solar distance). [B-3] The lever arm is the cross product of the sunline vector $\underline{S}''$ with the vector $\underline{Q}$ extending from the pressure center to the cg; it follows that the solar torque is

$$\underline{T}_s = \rho\left(\underline{Q} \times \underline{S}''\right) = \rho\left(\underline{Q} \times \underline{\underline{B}}^T \underline{S}\right) \qquad \text{(B-2)}$$

Fig. demonstrates the substitution of these torques into Euler's equations of motion. [B-4] Combined with various vector identities and simplifications in notation, these rotational equations are then rewritten (as suggested in Appendix A) in terms of the vehicle rates and known functions of the Euler angles. The specific relation between these angles and the vectors is given at the beginning of the next appendix.

APPENDIX C

EULER'S GEOMETRIC EQUATIONS

Figure shows the transformation from vehicle axes to the temporary inertial coordinates which correspond to time t_{m-1}. In accordance with equation (A-5), the sequence of rotations has the order (x,y,z); the expanded version of equation (A-5) is

$$\underline{\underline{G}} = \begin{bmatrix} \cos X_3 \cos X_2 & \sin X_3 \cos X_1 + \cos X_3 \sin X_2 \sin X_1 & \sin X_3 \sin X_1 - \cos X_3 \sin X_2 \cos X_1 \\ -\sin X_3 \cos X_2 & \cos X_3 \cos X_1 - \sin X_3 \sin X_2 \sin X_1 & \cos X_3 \sin X_1 + \sin X_3 \sin X_2 \cos X_1 \\ \sin X_2 & -\cos X_2 \sin X_1 & \cos X_2 \cos X_1 \end{bmatrix} \qquad \text{(C-1)}$$

The first expression for the angular rate vector $\underline{\omega}$ in figure , follows immediately from the diagram and the conventions adopted; from the diagram and equation (C-1) it also follows that

$$\underline{j}_1 = \underline{j} \cos X_1 + \underline{k} \sin X_1 \qquad \text{(C-2)}$$

and

$$\underline{k}_2 = \underline{k}_3 = \underline{i} \sin X_2 + \cos X_2 \left(-\underline{j} \sin X_1 + \underline{k} \cos X_1 \right) \qquad \text{(C-3)}$$

Collecting the coefficients of $\underline{i}$, $\underline{j}$, and $\underline{k}$,

$$\begin{bmatrix} X_4 \\ X_5 \\ X_6 \end{bmatrix} \triangleq \begin{bmatrix} \omega_1 \\ \omega_2 \\ \omega_3 \end{bmatrix} = \begin{bmatrix} -\dot{X}_1 - \dot{X}_3 \sin X_2 \\ -\dot{X}_2 \cos X_1 + \dot{X}_3 \sin X_1 \cos X_2 \\ -\dot{X}_3 \cos X_1 \cos X_2 - \dot{X}_2 \sin X_1 \end{bmatrix} \qquad \text{(C-4)}$$

and it can be verified by direct substitution that the position state variable derivatives are given by the expressions at the bottom of figure . In these expressions the appearance of the tangent and secant of (X_2) clearly illustrates the singularity which would arise if (X_2) were allowed to approach a right angle.

EULER'S GEOMETRIC EQUATIONS

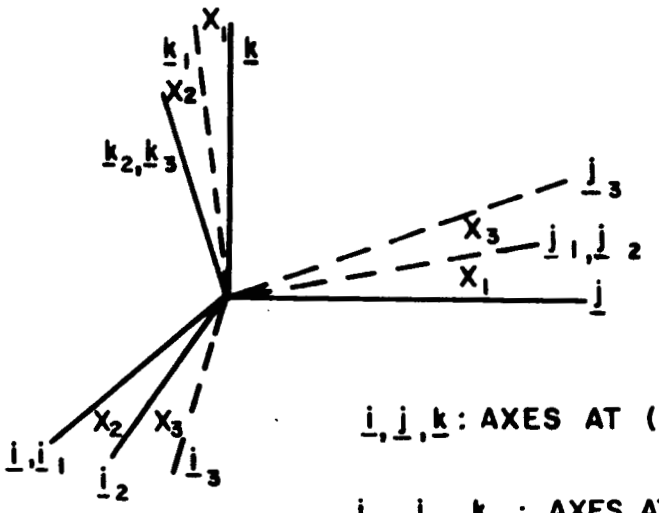

$\underline{i}, \underline{j}, \underline{k}$: AXES AT (t)

$\underline{i}_3, \underline{j}_3, \underline{k}_3$: AXES AT (t_{m-1})

$$\underline{\omega} = -\dot{X}_1\ \underline{i} - \dot{X}_2\ \underline{j}_1 - \dot{X}_3\ \underline{k}_3 ;$$

$$\underline{\omega} = -\dot{X}_1\ \underline{i} - \dot{X}_2 (\underline{j}\ \text{COS}\ X_1 + \underline{k}\ \text{SIN}\ X_1) - \dot{X}_3 \left[\underline{i}\ \text{SIN}\ X_2 + \text{COS}\ X_2 (-\underline{j}\ \text{SIN}\ X_1 + \underline{k}\ \text{COS}\ X_1)\right]$$

STATE VARIABLE FORM:

$$\dot{X}_1 = -X_4 + \text{TAN}\ X_2 (X_6\ \text{COS}\ X_1 - X_5\ \text{SIN}\ X_1)$$

$$\dot{X}_2 = -X_5\ \text{COS}\ X_1 - X_6\ \text{SIN}\ X_1$$

$$\dot{X}_3 = -\text{SEC}\ X_2 (X_6\ \text{COS}\ X_1 - X_5\ \text{SIN}\ X_1)$$

APPENDIX D

RESTRICTIVE SOLUTION TO EULER'S EQUATIONS

For a torque-free satellite with dynamical symmetry about its x-axis (i.e., $I_2 = I_3 = I$), Euler's equations of motion reduce to

$$\dot{\omega}_1 = 0 \; ; \; I\dot{\omega}_2 = -(I_1 - I)\omega_1\omega_3 \; ; \; I\dot{\omega}_3 = (I_1 - I)\omega_1\omega_2 \qquad \text{(D-1)}$$

The solution to these equations can readily be expressed in terms of a spin rate (ω_A), a retrograde* precession rate (ω_B), the angle (α) between the spin axis ($\underline{i}$) and the angular momentum vector ($\underline{h}$); and a spin phase angle ($\omega_A t_A$). These constants are defined by the initial angular rate vector $\underline{\omega}_o$ as follows:

$$\omega_A = -\xi\omega_{01} \qquad \text{(D-2)}$$

$$\omega_B = I_1\omega_A \sec\alpha/(I_1 - I) = -(I_1/I)\omega_{01}\sec\alpha \qquad \text{(D-3)}$$

$$\alpha = \text{Arctan}\{I\omega_{yz}/I_1\omega_{01}\}, \quad 0 \leq \alpha \leq \pi \qquad \text{(D-4)}$$

$$\omega_A t_A = \arctan(\omega_{02}\,;\,\omega_{03}) \qquad \text{(D-5)}$$

where

$$\xi \triangleq (I_1 - I)/I \qquad \text{(D-6)}$$

$$\omega_{yz} \triangleq +\sqrt{\omega_{02}^2 + \omega_{03}^2} \qquad \text{(D-7)}$$

and the double argument inverse tangent of (D-5) is defined as the inverse tangent of the ratio (ω_{02}/ω_{03}) with the quadrant dictated by the algebraic signs of the numerator and the denominator. In terms of these constants, the solution to (D-1) may be written as

$$\omega_1 = \omega_{01} = -\omega_A/\xi \qquad \text{(D-8)}$$

$$\omega_2 = -A_s\omega_A(\xi+1)\tan\alpha/\xi \qquad \text{(D-9)}$$

$$\omega_3 = -A_c\omega_A(\xi+1)\tan\alpha/\xi \qquad \text{(D-10)}$$

in which (A_s) and (A_c) are defined as the sine and cosine, respectively, of the

*The case ($I_1 > I$), corresponding to spin stabilization about the major principal axis, is typical of most space applications.

composite angle $\omega_A(t+t_A)$. It is also noted that

$$\omega_2 = \omega_{02}\cos(\xi\omega_1 t) - \omega_{03}\sin(\xi\omega_1 t) \qquad \text{(D-11)}$$

$$\omega_3 = \omega_{02}\sin(\xi\omega_1 t) + \omega_{03}\cos(\xi\omega_1 t) \qquad \text{(D-12)}$$

This formulation corresponds to the XYX Euler angle sequence,

$$\underline{\underline{\eta}} \triangleq \left[\omega_B t\right]_x \left[-\alpha\right]_y \left[-\omega_A(t+t_A)\right]_x \qquad \text{(D-13)}$$

and it can easily be verified that the derivative of this matrix is equal to the product,

$$\dot{\underline{\underline{\eta}}} = \begin{bmatrix} \alpha_c & \alpha_s A_s & \alpha_s A_c \\ -\alpha_s B_s & A_c B_c + \alpha_c A_s B_s & -A_s B_c + \alpha_c A_c B_s \\ -\alpha_s B_c & -A_c B_s + \alpha_c A_s B_c & A_s B_s + \alpha_c A_c B_c \end{bmatrix} \begin{bmatrix} 0 & \alpha_s \omega_B A_c & -\alpha_s \omega_B A_s \\ -\alpha_s \omega_B A_c & 0 & -\omega_A + \alpha_c \omega_B \\ \alpha_s \omega_B A_s & \omega_A - \alpha_c \omega_B & 0 \end{bmatrix} \qquad \text{(D-14)}$$

where the subscripts (s,c) again denote the sine and cosine, respectively, of the angles contained in (D-13). The correspondence between the off-diagonal terms of the above skew-symmetric matrix and the angular rates of (D-8) to (D-10) is easily established from the defining relationships given earlier. It follows that the premultiplying factor on the right of (D-14) is a closed form solution for vehicle attitude, complete to within a premultiplicative* constant matrix. Obviously, to satisfy the initial conditions, the complete transformation from vehicle to inertial co-ordinates must be

$$\underline{\underline{B}} = \underline{\underline{B}}_R \left[\omega_A t_A\right]_x \left[\alpha\right]_y \left[\omega_B t\right]_x \left[-\alpha\right]_y \left[-\omega_A(t+t_A)\right]_x \qquad \text{(D-15)}$$

*Postmultiplication of $\underline{\underline{\eta}}$ by a constant matrix would destroy the differential equation relationship for a transformation from vehicle to stabilized co-ordinates.

where $\underline{\underline{B}}_R$ is the value of $\underline{\underline{B}}$ at the reference time.

The following comments will facilitate a rigorous interpretation of the preceding analysis:

(1) The angular momentum vector in vehicle co-ordinates,

$$\underline{h} = \underline{i}\, I_1 \omega_1 + I\left(\underline{j}\,\omega_2 + \underline{k}\,\omega_3\right) \qquad \text{(D-16)}$$

has a magnitude of ($I_1 \omega_{01} \sec \alpha$). The conventions adopted here ensure that, since (ω_{01}) and ($\sec\alpha$) always have the same sign, this expression cannot of course be negative. It is easily verified that ($\underline{\underline{\eta}}\,\underline{h}$) has only an x - component.

(2) The phase angle $\omega_A t_A$ is equal to the angle between $\underline{h}$ and the initial $\underline{k}$ axis. By including this in the transformation, it is insured that the intermediate y-axis is indeed perpendicular to the plane of $\underline{h}$ and the initial vehicle x-axis. This paves the way for the middle transformation in (D-13).

(3) By definition, the algebraic signs of (ω_{01}) and ($\cos\alpha$) must agree. From (D-2) it follows that, when ($\mathcal{F}$) is positive, (ω_A) is positive for obtuse (α) and negative for actue (α). From (D-3) it can be seen that ω_B always turns out negative with the conventions adopted here.* Since the spin and precession rates are of opposite sense in (D-13), it follows that positive values of ($\mathcal{F}$) produce retrograde precession.

(4) Force-free precession is described in various other references. [D-1, D-2] The solution given here for vehicle rates, attitude matrices, pertinent constants, and all angles, must be regarded as well known. It has been included here under a unified notation in order to provide a complete background for the next section (Appendix E).

*This could have been changed by redefining (α), restricting its value to acute angles, or by one of several alternate formulations. The matrix solution, however, would have to remain unchanges.

APPENDIX E

PRECESSION OF ANGULAR MOMENTUM BY SMALL TORQUES

For certain symmetrical spinning satellites under consideration in this study, a solar pressure model described in recent literature [E-1] is applicable. When gravity gradient is absent (as is essentially true of solar orbiters or satellites at ten earth radii), a substantially* regular precession rate of

$$\omega_p = (\cos^2 \alpha) P_\rho A_v q / (I_1 \omega_1) \qquad \text{(E-1)}$$

acts upon the angular momentum vector. In this case, the transformation matrix $\underline{\underline{B}}$ generalizes to

$$\underline{\underline{B}} = \underline{\underline{B}}_0 \left[\omega_A t_A\right]_x \left[\alpha\right]_y \left[\alpha_{kv} - \omega_A t_A\right]_x \left[\alpha_{hv}\right]_y \left[-\omega_p t\right]_x \left[-\alpha_{hv}\right]_y \left[\omega_A t_A - \alpha_{kv}\right]_x \underline{\underline{\eta}} \qquad \text{(E-2)}$$

where (α_{kv}) is the angle between the initial yaw axis orientation and the reference line $\underline{V}$;

$$\alpha_{kv} = sgn(\underline{B}_2 \cdot \underline{V}) \operatorname{Arccos}(\underline{B}_3 \cdot \underline{V}) \qquad \text{(E-3)}$$

and (α_{hv}) is the angle between $\underline{V}$ and the initial angular momentum vector,

$$\alpha_{hv} = \operatorname{Arccos}\left\{\left[I_1 \omega_{01} v_1'' + I(\omega_{02} v_2'' + \omega_{03} v_3'')\right] / (I_1 \omega_{01} \sec \alpha)\right\} \; ; \; 0 \leq \alpha_{hv} \leq \pi \qquad \text{(E-4)}$$

In this case $\underline{V}$ represents the sunline in inertial co-ordinates and $\underline{V}''$ is the same vector transformed through $\underline{\underline{B}}_0$. Equation (E-2) of course reduces to (D-15) when ω_p vanishes. Also, when ω_p is not zero but (α) vanishes, (E-2) reduces to a form quite similar to (D-15); the analogy is nearly self-explanatory.

When no solar torque is present (e.g., if q = 0), the last three equations are applicable with $\underline{V}$ redefined as the orbit pole vector and [E-2]

$$\omega_p = -(3/2) n_o^2 \cos \alpha_{hv} \cos \alpha \left[1 - \frac{3}{2} \sin^2 \alpha\right] \xi / \left[(1+\xi) \omega_{01}\right] \qquad \text{(E-5)}$$

*This formulation is incomplete for simulations of flight duration exceeding one million seconds; the sunline must remain reasonably fixed in inertial space.

APPENDIX F

LIBRATION OF VERTICALLY ORIENTED SATELLITES

The immediate discussion will be limited to rigid satellites with no active or passive control torques and, for reasons which will be clear shortly, only circular orbits will be considered.

A non-spinning satellite can be locally stabilized by a gravity gradient torque which tends to align its yaw axis with the vertical* (see Appendix B). Stable motion of this type is characterized by an inertial angular velocity which is nearly equal to the orbital rate, having a direction which nearly coincides with the pitch axis. By linearizing Euler's equations for these conditions, approximate solutions describing the satellite angular motion can be obtained in closed form.[F-1] However, while this is valid for sufficiently small displacements from the reference orientation, the technique is subject to some unexpectedly severe restrictions.[F-2] In the general case of three unequal principal moments of inertia, stability is unexpectedly sensitive, even for circular orbits.** Since orbit ellipticity would further inhibit the stability, elliptical orbits are not treated analytically. In general, no effort is made to use linearization techniques except in conjunction with those conditions for which the stability restrictions are known.

---

*This is not the only stabilizing mode for gravity gradient torque, but it is of primary interest here.

**It is of interest to note that bounded (and therefore, stable) motion can be demonstrated by true nonlinear analysis in the symmetrical case.[F-3] In following the derivation given in Ref. (F-3) it is important to note that the energy integral is the Hamiltonian function, which is not equal to the total energy. This latter point is explained in an extended analysis along similar lines.[F-4]

For small angular displacements from reference local co-ordinates, the following approximations are introduced:

$$\underline{\underline{C}} \doteq \begin{bmatrix} 1 & \delta_3 & -\delta_2 \\ -\delta_3 & 1 & \delta_1 \\ \delta_2 & -\delta_1 & 1 \end{bmatrix} \tag{F-1}$$

$$\begin{bmatrix} \dot{\delta}_1 \\ \dot{\delta}_2 \\ \dot{\delta}_3 \end{bmatrix} \doteq \begin{bmatrix} -\omega_1 - \delta_3 \eta_0 \\ -\omega_2 + \eta_0 \\ -\omega_3 + \delta_1 \eta_0 \end{bmatrix} \tag{F-2}$$

Substituting these into Euler's equations of motion, retaining only first order terms,

$$I_1 \ddot{\delta}_1 + (I_3 + I_1 - I_2)\eta_0 \dot{\delta}_3 - 4(I_3 - I_2)\eta_0^2 \delta_1 = 0 \tag{F-3}$$

$$I_2 \ddot{\delta}_2 + 3(I_1 - I_3)\eta_0^2 \delta_2 = 0 \tag{F-4}$$

$$I_3 \ddot{\delta}_3 - (I_3 + I_1 - I_2)\eta_0 \dot{\delta}_1 + (I_2 - I_1)\eta_0^2 \delta_3 = 0 \tag{F-5}$$

These expressions are equivalent to Eqs. (I) of Ref. (F-1), permuted and modified by appropriate notation changes. A restrictive closed form solution for small oscillations can be applied under the conditions summarized below:

(1) Only earth satellites are considered.

(2) No solar torque can be present.

(3) The orbit must be circular.

(4) Only small initial angular displacements are allowed; $(z_1^2 + z_2^2 + z_3^2)^{1/2} < 0.1$.

(5) For stability of vertical orientation, $I_1 > I_3$.

(6) The stability conditions in Ref. (F-1) must be satisfied*:

$$\xi_1 \xi_3 < 0 \; ; \; F_1 = (1 - 3\xi_1 - \xi_1 \xi_3) > 0 \; ; \; F_2 = F_1^2 + 16\xi_1 \xi_3 > 0 \tag{F-6}$$

* ξ are defined in Fig.

(7) Only small initial values are allowed for the derivative ($\dot{\delta}_2$):

$$|\omega_{02} - \eta_0| \leq 0.1 \sqrt{3\xi_2}\,\eta_0 \qquad \text{(F-7)}$$

and the initial rates ($\dot{\delta}_1$, $\dot{\delta}_3$) must be negligible*;

$$|\omega_{01} + \eta_0 \gamma_3| < 0.01 (\Lambda_1 Z_{11} + \Lambda_2 Z_{21}) \qquad \text{(F-8)}$$

$$|\omega_{03} - \eta_0 \gamma_1| < 0.01 (\Lambda_1 Z_{13} + \Lambda_2 Z_{23}) \qquad \text{(F-9)}$$

where

$$\Lambda_1 = \eta_0 \sqrt{F_1 + \sqrt{F_2}} \quad ; \quad \Lambda_2 = \eta_0 \sqrt{F_1 - \sqrt{F_2}} \qquad \text{(F-10)}$$

and

$$Z_{11} = \left[(R_{11}\gamma_1)^2 + (R_{31}\gamma_3)^2 \right]^{1/2} \; ; \; Z_{21} = \left[(R_{21}\gamma_1)^2 + (R_{41}\gamma_3)^2 \right]^{1/2} \qquad \text{(F-11)}$$

$$Z_{13} = \left[(R_{33}\gamma_1)^2 + (R_{13}\gamma_3)^2 \right]^{1/2} \; ; \; Z_{23} = \left[(R_{43}\gamma_1)^2 + (R_{23}\gamma_3)^2 \right]^{1/2} \qquad \text{(F-12)}$$

with the R-parameters defined as

$$\begin{bmatrix} R_{11} \\ R_{21} \\ R_{31} \\ R_{41} \end{bmatrix} = \frac{1}{\Lambda_1^2 - \Lambda_2^2} \begin{bmatrix} \Lambda_1^2 - \eta_0^2 (1 + \xi_1 - \xi_1 \xi_3) \\ \Lambda_2^2 - \eta_0^2 (1 + \xi_1 - \xi_1 \xi_3) \\ (1 + \xi_1) \xi_3 \eta_0^3 / \Lambda_1 \\ (1 + \xi_1) \xi_3 \eta_0^3 / \Lambda_2 \end{bmatrix} \qquad \text{(F-13)}$$

$$\begin{bmatrix} R_{13} \\ R_{23} \\ R_{33} \\ R_{43} \end{bmatrix} = \frac{1}{\Lambda_1^2 - \Lambda_2^2} \begin{bmatrix} \Lambda_1^2 - \eta_0^2 (1 - \xi_3 - 5\xi_1 + \xi_1 \xi_3) \\ \Lambda_2^2 - \eta_0^2 (1 - \xi_3 - 5\xi_1 + \xi_1 \xi_3) \\ 4(1 - \xi_3) \xi_1 \eta_0^3 / \Lambda_1 \\ 4 (1 - \xi_3) \xi_1 \eta_0^3 / \Lambda_2 \end{bmatrix} \qquad \text{(F-14)}$$

* This is not an essential restriction. It was adopted to simplify the analytical form without unduly limiting its scope.

(8) All amplitudes (Z) are restricted to values below one-tenth radian. This limitation was chosen because of the plurality of unstable points in Figs. 8 and 9 of Ref. (F-2).

When the above eight conditions are satisfied, the angular displacement from the local reference can be closely approximated by uncoupled pitch oscillations,

$$\delta_2 = \left[Z_2^2 + (\dot{\delta}_{02})^2 / 3\xi_2 \eta_0^2 \right]^{1/2} \cos\left\{ \sqrt{3\xi_2}\, \eta_0 t + \Psi_2 \right\} \qquad \text{(F-15)}$$

and coupled yaw-roll oscillations,

$$\delta_1 = Z_{11} \cos(\eta_1 t + \Psi_{11}) - Z_{21} \cos(\eta_2 t + \Psi_{21}) \qquad \text{(F-16)}$$

$$\delta_3 = Z_{13} \cos(\eta_1 t + \Psi_{13}) - Z_{23} \cos(\eta_2 t + \Psi_{23}) \qquad \text{(F-17)}$$

where (see Appendix D for a definition of the double argument inverse tangent)

$$\Psi_2 = \arctan\left\{ \dot{\delta}_{02} \,;\, \sqrt{3\xi_2}\, \eta_0 Z_2 \right\} \qquad \text{(F-18)}$$

$$\Psi_{11} = \arctan\left\{ -R_{31} Z_3 \,;\, R_{11} Z_1 \right\} \qquad \text{(F-19)}$$

$$\Psi_{21} = \arctan\left\{ -R_{41} Z_3 \,;\, R_{21} Z_1 \right\} \qquad \text{(F-20)}$$

$$\Psi_{13} = \arctan\left\{ -R_{33} Z_1 \,;\, R_{13} Z_3 \right\} \qquad \text{(F-21)}$$

$$\Psi_{23} = \arctan\left\{ -R_{43} Z_1 \,;\, R_{23} Z_3 \right\} \qquad \text{(F-22)}$$

These closed form expressions are programmed as an independent check for the numerical integration of Euler's equations.

APPENDIX G

STATE VARIABLE EQUATIONS

The state variable forms of Euler's dynamic and geometric equations are given in Figs. and , respectively. In addition to integrating these true equations of motion, the simulation determines the apparent state from the following relations:

$$\begin{bmatrix} \dot{\hat{X}}_1 \\ \dot{\hat{X}}_2 \\ \dot{\hat{X}}_3 \\ \dot{\hat{X}}_4 \\ \dot{\hat{X}}_5 \\ \dot{\hat{X}}_6 \end{bmatrix} = \begin{bmatrix} -\hat{X}_4 + \tan\hat{X}_2\left(\hat{X}_6\cos\hat{X}_1 - \hat{X}_5\sin\hat{X}_1\right) \\ -\hat{X}_5\cos\hat{X}_1 - \hat{X}_6\sin\hat{X}_1 \\ -\sec\hat{X}_2\left(\hat{X}_6\cos\hat{X}_1 - \hat{X}_5\sin\hat{X}_1\right) \\ \varepsilon_1\left[-\hat{X}_5\hat{X}_6 + 3\mu(\hat{\underline{\Gamma}}_3)^T\hat{\underline{G}}_3(\hat{\underline{\Gamma}}_3)^T\hat{\underline{G}}_2/r^3\right] + \nu_{21}(\hat{\underline{G}}_3)^T\hat{\underline{S}}' - \nu_{31}(\hat{\underline{G}}_2)^T\hat{\underline{S}}' \\ \varepsilon_2\left[-\hat{X}_6\hat{X}_4 + 3\mu(\hat{\underline{\Gamma}}_3)^T\hat{\underline{G}}_1(\hat{\underline{\Gamma}}_3)^T\hat{\underline{G}}_3/r^3\right] + \nu_{32}(\hat{\underline{G}}_1)^T\hat{\underline{S}}' - \nu_{12}(\hat{\underline{G}}_3)^T\hat{\underline{S}}' \\ \varepsilon_3\left[-\hat{X}_4\hat{X}_5 + 3\mu(\hat{\underline{\Gamma}}_3)^T\hat{\underline{G}}_2(\hat{\underline{\Gamma}}_3)^T\hat{\underline{G}}_1/r^3\right] + \nu_{13}(\hat{\underline{G}}_2)^T\hat{\underline{S}}' - \nu_{23}(\hat{\underline{G}}_1)^T\hat{\underline{S}}' \end{bmatrix} \qquad (G\text{-}1)$$

where $\hat{X}_i$, $\dot{\hat{X}}_i$ denote the instantaneous observed state variable and its first time derivative, as determined by the simulated attitude tracking data processor; $\hat{\underline{G}}_i$ is the (ith) column of the orthogonal matrix,

$$\hat{\underline{\underline{G}}} = [\hat{X}_3]_z[\hat{X}_2]_y[\hat{X}_1]_x \qquad (G\text{-}2)$$

$\hat{\underline{\Gamma}}_i$ is the (ith) column of the orthogonal matrix,

$$\underline{\underline{\Gamma}} = \left(\hat{\underline{\underline{C}}}_{m-1}\right)^T\begin{bmatrix}0&1&0\\0&0&1\\1&0&0\end{bmatrix}[\theta_{m-1} - \theta]_z\begin{bmatrix}0&0&1\\1&0&0\\0&1&0\end{bmatrix} \qquad (G\text{-}3)$$

and

$$\hat{\underline{S}}' = \left(\hat{\underline{\underline{B}}}_{m-1}\right)^T\underline{S} \qquad (G\text{-}4)$$

Note that $\hat{\underline{\underline{\Gamma}}}$ and $\hat{\underline{S}}'$ both are independent time varying functions, since they involve only (1) the known observed attitudes in the past and (2) translational

navigation and ephemeris data which can be assumed known from independent sources. It follows that equation (G-1) represents the state variable relationship which can be used in the physical system to obtain the transition properties derived below.

APPENDIX H

STATE TRANSITION MATRIX

The state variable equations are of the form,

$$d\underline{X}/dt = \dot{\underline{X}}(X_1, X_2, \cdots X_6, t) \tag{H-1}$$

Partial differentiation with respect to the state variables which correspond to time t_o can be written symbolically as

$$\partial\dot{\underline{X}}/\partial X_0 = \left[\partial\dot{\underline{X}}/\partial\underline{X}\right]\left[\partial\underline{X}/\partial\underline{X}_0\right] \tag{H-2}$$

Interchanging the order of differentiation on the left side,

$$\dot{\underline{\underline{\Phi}}} = \underline{\underline{A}}\,\underline{\underline{\Phi}} \tag{H-3}$$

where

$$\underline{\underline{\Phi}} \triangleq \partial\underline{X}/\partial\underline{X}_0 \tag{H-4}$$

and

$$\underline{\underline{A}} \triangleq \partial\dot{\underline{X}}/\partial\underline{X} \tag{H-5}$$

The state transition matrix is the solution of (H-3) subject to the initial conditions,

$$\underline{\underline{\Phi}}(0) = \underline{\underline{I}}_{66} \tag{H-6}$$

Observed quantities are used throughout because the physical system will always use the updated estimate as the reference.

As a step in determining the A-matrix, it is convenient to write the last three state equations as

$$\hat{\ddot{X}}_{i+3} = f_i\left[-\hat{\omega}_{i+1}\hat{\omega}_{i+2} + 3\mu(\hat{\underline{r}}_3)^T\hat{\underline{G}}_{i+2}(\hat{\underline{r}}_3)^T\hat{\underline{G}}_{i+1}/r^3\right] + \tag{H-7}$$

$$\nu_{i+1,i}(\hat{\underline{G}}_{i+2})^T\hat{\underline{S}}' - \nu_{i+2,i}(\hat{\underline{G}}_{i+1})^T\hat{\underline{S}}' \quad ; \quad i,j = 1,2,3$$

from which it follows that

$$a_{i+3,j} = (3\mu f_i/r^3)(\hat{\underline{r}}_3)^T\left[\hat{\underline{G}}_{i+2}(\hat{\underline{r}}_3)^T\frac{\partial\hat{\underline{G}}_{i+1}}{\partial\hat{X}_j} + \frac{\partial\hat{\underline{G}}_{i+2}}{\partial\hat{X}_j}(\hat{\underline{r}}_3)^T\hat{\underline{G}}_{i+1}\right] \tag{H-8}$$

$$+\left[\nu_{i+1,i}\left(\frac{\partial\hat{\underline{G}}_{i+2}}{\partial\hat{X}_j}\right)^T - \nu_{i+2,i}\left(\frac{\partial\hat{\underline{G}}_{i+1}}{\partial\hat{X}_j}\right)^T\right]\hat{\underline{S}}'$$

where the vectors ($\partial \underline{G}_n / \partial \hat{X}_j$) follow from equation (C-1);

$$\left[\partial \hat{\underline{\underline{G}}} / \partial \hat{X}_1\right] = \left[\underline{0}_{31} \;,\; -\hat{\underline{G}}_3 \;,\; \hat{\underline{G}}_2\right] \tag{H-9}$$

$$\left[\partial \hat{\underline{\underline{G}}} / \partial \hat{X}_2\right] = \left[\hat{\underline{G}}_3 \cos\hat{X}_1 - \hat{\underline{G}}_2 \sin\hat{X}_1 \;,\; \hat{\underline{G}}_1 \sin\hat{X}_1 \;,\; -\hat{\underline{G}}_1 \cos\hat{X}_1\right] \tag{H-10}$$

$$\left[\partial \hat{\underline{\underline{G}}} / \partial \hat{X}_3\right] = \left[\hat{\underline{G}}_1 \times \underline{1}_3 \;,\; \hat{\underline{G}}_2 \times \underline{1}_3 \;,\; \hat{\underline{G}}_3 \times \underline{1}_3\right] \tag{H-11}$$

In equation (H-11), $\underline{1}_3$ is the column vector consisting of the components (0,0,1).

Aside from this lower left submatrix, the other elements follow from inspection of the state equations. The complete matrix is

$$\underline{\underline{A}} = \begin{bmatrix}
\dot{\hat{X}}_2 \tan\hat{X}_2 & -\dot{\hat{X}}_3 \sec\hat{X}_2 & 0 & -1 & -\tan\hat{X}_2 \sin\hat{X}_1 & \tan\hat{X}_2 \cos\hat{X}_1 \\
\dot{\hat{X}}_3 \cos\hat{X}_2 & 0 & 0 & 0 & -\cos\hat{X}_1 & -\sin\hat{X}_1 \\
-\dot{\hat{X}}_2 \sec\hat{X}_2 & \dot{\hat{X}}_3 \tan\hat{X}_2 & 0 & 0 & \sec\hat{X}_2 \sin\hat{X}_1 & -\sec\hat{X}_2 \cos\hat{X}_1 \\
a_{41} & a_{42} & a_{43} & 0 & -\xi_1 \hat{X}_6 & -\xi_1 \hat{X}_5 \\
a_{51} & a_{52} & a_{53} & -\xi_2 \hat{X}_6 & 0 & -\xi_2 \hat{X}_4 \\
a_{61} & a_{62} & a_{63} & -\xi_3 \hat{X}_5 & -\xi_3 \hat{X}_4 & 0
\end{bmatrix} \tag{H-12}$$

In the special case of zero torque and one axis of dynamic symmetry, the transition matrix can be obtained in closed form. The lower half is especially straightforward, following from inspection of equations (D-8), (D-11), and (D-12). The upper half is approached by generalizing equation (A-5) to allow finite (nonzero) values of the initial Euler angles;

$$\left[X_3\right]_z \left[X_2\right]_y \left[X_1\right]_x = \left[X_{03}\right]_z \left[X_{02}\right]_y \left[X_{01}\right]_x \underline{\underline{G}} \tag{H-13}$$

Defining the partial derivative matrices for $1 < j < 3$,

$$\left[\nabla_j X_1\right] = \begin{bmatrix} 0 & 0 & 0 \\ 0 & -X_{1S} & X_{1C} \\ 0 & -X_{1C} & -X_{1S} \end{bmatrix} \phi_{1j} \tag{H-14}$$

$$\left[\nabla_j X_2\right] = \begin{bmatrix} -X_{2S} & 0 & -X_{2C} \\ 0 & 0 & 0 \\ X_{2C} & 0 & -X_{2S} \end{bmatrix} \phi_{2j} \tag{H-15}$$

$$\left[\nabla_j X_3\right] = \begin{bmatrix} -X_{3S} & X_{3C} & 0 \\ -X_{3C} & -X_{3S} & 0 \\ 0 & 0 & 0 \end{bmatrix} \phi_{3j} \tag{H-16}$$

with (s) and (c) denoting sine and cosine, respectively, (H-13) can be differentiated thus*:

$$\left[\nabla_j X_3\right]\left[X_2\right]_y\left[X_1\right]_x + \left[X_3\right]_z\left[\nabla_j X_2\right]\left[X_1\right]_x + \left[X_3\right]_z\left[X_2\right]_y\left[\nabla_j X_1\right] = \tag{H-17}$$

$$\begin{bmatrix} 0 & \delta_{3j} & -\delta_{2j} \\ -\delta_{3j} & 0 & \delta_{1j} \\ \delta_{2j} & -\delta_{1j} & 0 \end{bmatrix} \equiv \underline{\underline{G}}$$

where (δ_{ij}) is the Kronecker delta function. This can be rewritten as

$$\begin{bmatrix} -g_{21} & -g_{22} & -g_{23} \\ g_{11} & g_{12} & g_{13} \\ 0 & 0 & 0 \end{bmatrix} \phi_{3j} + \begin{bmatrix} X_{1S}g_{12} - X_{1C}g_{13} & -X_{1S}g_{11} & X_{1C}g_{11} \\ X_{1S}g_{22} - X_{1C}g_{23} & -X_{1S}g_{21} & X_{1C}g_{21} \\ X_{1S}g_{32} - X_{1C}g_{33} & -X_{1S}g_{31} & X_{1C}g_{31} \end{bmatrix} \phi_{2j} +$$

$$\begin{bmatrix} 0 & g_{13} & -g_{12} \\ 0 & g_{23} & -g_{22} \\ 0 & g_{33} & -g_{32} \end{bmatrix} \phi_{1j} = \begin{bmatrix} 0 & -\delta_{3j} & \delta_{2j} \\ \delta_{3j} & 0 & -\delta_{1j} \\ -\delta_{2j} & \delta_{1j} & 0 \end{bmatrix} \equiv \underline{\underline{G}} \tag{H-18}$$

*Equation (H-17) contains the special case conditions $X_{01}=X_{02}=X_{03}=0$, substituted into the matrix equations <u>after</u> differentiation.

It can easily be verified that this matrix relation is satisfied (under conditions of equations C-1 and H-6) by

$$\begin{bmatrix} \phi_{11} & \phi_{12} & \phi_{13} \\ \phi_{21} & \phi_{22} & \phi_{23} \\ \phi_{31} & \phi_{32} & \phi_{33} \end{bmatrix} = \begin{bmatrix} \cos X_3 \sec X_2 & -\sin X_3 \sec X_2 & 0 \\ \sin X_3 & \cos X_3 & 0 \\ -\cos X_3 \tan X_2 & \sin X_3 \tan X_2 & 1 \end{bmatrix} \qquad \text{(H-19)}$$

All that remains is the submatrix $(\partial X_i / \partial \omega_{oj})$ for $1 < i < 3$, which can be determined from a combination of equations (C-1) and the identification of $\underline{\underline{G}}$ per Appendix D:

$$\underline{\underline{G}} = \left[\omega_A t_A\right]_x \left[\alpha\right]_y \left[\omega_B t\right]_x \left[-\alpha\right]_y \left[-\omega_A (t+t_A)\right]_x \qquad \text{(H-20)}$$

From the elements g_{11}, g_{21}, g_{31}, g_{32}, and g_{33} of (C-1) it follows that

$$\partial X_1 / \partial \omega_{oj} = -(g_{33} \nabla_j g_{32} - g_{32} \nabla_j g_{33}) \sec^2 X_2 \qquad \text{(H-21)}$$

$$\partial X_2 / \partial \omega_{oj} = (\nabla_j g_{31}) \sec X_2 \qquad \text{(H-22)}$$

$$\partial X_3 / \partial \omega_{oj} = -(g_{11} \nabla_j g_{21} - g_{21} \nabla_j g_{11}) \sec^2 X_2 \qquad \text{(H-23)}$$

where $\nabla_j (g_{mn}) \triangleq \partial g_{mn} / \partial \omega_{oj}$ with elements taken from (H-20),

$$g_{11} = \alpha_c^2 (1 - B_c) + B_c \qquad \text{(H-24)}$$

$$g_{21} = \alpha_s \alpha_c k_s (1 - B_c) - \alpha_s k_c B_s \qquad \text{(H-25)}$$

$$g_{31} = \alpha_s \alpha_c k_c (1 - B_c) + \alpha_s k_s B_s \qquad \text{(H-26)}$$

$$g_{32} = A_s(\alpha_s^2 k_c + \alpha_c^2 k_c B_c - \alpha_c k_s B_s) - A_c(k_s B_c + \alpha_c k_c B_s) \qquad \text{(H-27)}$$

$$g_{33} = A_c(\alpha_s^2 k_c + \alpha_c^2 k_c B_c - \alpha_c k_s B_s) + A_s(k_s B_c + \alpha_c k_c B_s) \qquad \text{(H-28)}$$

in which, finally, (k_s) and (k_c) are defined as the sine and cosine, respectively, of the phase angle ($\omega_A t_A$) and the remaining subscripted quantities above are defined as in Appendix D.

It should be noted that, in the simulation, all transition matrix elements are computed from observed parameters. (The usual circumflex notation was omitted above, merely to facilitate the presentation.)

APPENDIX I

KALMAN FILTER EQUATIONS*

The minimum variance data processing equations are based upon a linearized representation of the transition from the state at the time of the last (m-1) measurement to the current (m) measurement time,

$$\underline{x}_m = \underline{\underline{\Phi}}_m \, \underline{x}_{m-1} \tag{I-1}$$

and the relations between observable and state are linearized thus:

$$\underline{y}_m = \underline{H}_m \, \underline{x}_m \tag{I-2}$$

For a state uncertainty covariance $\underline{\underline{P}}$ and a measurement variance σ_m^2 it has been shown [I-1] that the minimum variance estimator can be computed recursively as

$$\underline{X}^{(+)} = \underline{X}^{(-)} + \underline{W} \, \hat{y} \tag{I-3}$$

where the superscripts (-) and (+) stand for immediately before and after the measurement, respectively, and

$$\underline{W} = \underline{\underline{P}} \, \underline{H}^T \left[\underline{H} \, \underline{\underline{P}} \, \underline{H}^T + \sigma_m^2 \right]^{-1} \tag{I-4}$$

The current measurement produces a step reduction in uncertainty

$$\underline{\underline{P}}^{(+)} = \left[\underline{\underline{I}}_{66} - \underline{W} \, \underline{H} \right] \underline{\underline{P}}^{(-)} \tag{I-5}$$

and, between measurements, the uncertainty covariance matrix is extrapolated by the relation

$$\underline{\underline{P}}_m^{(-)} = \underline{\underline{\Phi}}_m \, \underline{\underline{P}}_{m-1}^{(+)} \, \underline{\underline{\Phi}}_m^T \tag{I-6}$$

Initial conditions for $\underline{\underline{P}}$ are provided by assuming a diagonal matrix with typical values of initial estimation error for angles and their rates. It has been shown that the diagonal matrix assumption is conservative. [I-2, I-3]

*The expressions in this section are specialized to the case of independent scalar measurements.

APPENDIX J

SUNLINE MEASUREMENTS AND SENSITIVITIES

Fig. illustrates a sun sensor instrument face (normal to $\underline{L}_1$) with a slit (along the direction of $\underline{U}$) having a field of view such that, if

$$\underline{S}'' \cdot \underline{L}_{1n} > \cos 64^\circ \tag{J-1}$$

then the angle (γ) will be directly measureable. The last expression of Fig. can be written as

$$\cos\gamma = (\underline{S}')^T \underline{\underline{G}}\, \underline{L} \Big/ \left\{1 - \left[(\underline{S}')^T \underline{\underline{G}}\, \underline{U}\right]^2\right\}^{1/2} \tag{J-2}$$

Taking variations in the observable and state,

$$-\sin\gamma\, \delta\gamma = (1/\sin^2\zeta)\left\{|\sin\zeta|(\underline{S}')^T \left[\sum_i (\partial \underline{\underline{G}}/\partial X_i)\delta X_i\right]\underline{L} + (\underline{S}')^T \underline{\underline{G}}\, \underline{L} |\sin\zeta|^{-1} \cos\zeta\, (\underline{S}')^T \left[\sum_i (\partial \underline{\underline{G}}/\partial X_i)\delta X_i\right]\underline{U}\right\} \tag{J-3}$$

or

$$\delta\gamma = (-1/\sin^2\zeta \sin\gamma)(\underline{S}')^T \left[\sum_i (\partial \underline{\underline{G}}/\partial X_i)\delta X_i\right]\underline{N} \tag{J-4}$$

SUN SENSOR

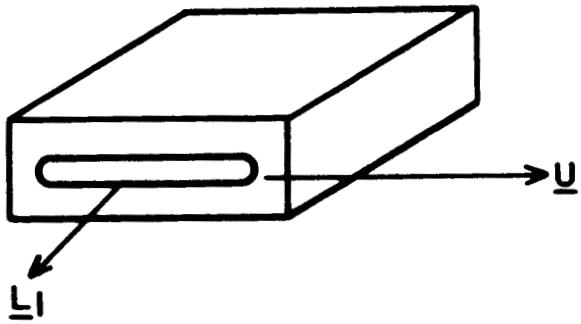

ADDITIONAL VECTORS

$$\underline{S}'' \triangleq \underline{\underline{B}}^T \underline{S} = \underline{\underline{G}}^T \underline{S}'$$

$$\underline{V} \triangleq \frac{\underline{S}'' \times \underline{U}}{|\underline{S}'' \times \underline{U}|} = \frac{\underline{S}' \times \underline{\underline{G}}\, \underline{U}}{|\underline{S}' \times \underline{\underline{G}}\, \underline{U}|}$$

MEASURED ANGLE = $Y = \arccos(\underline{V} \cdot \underline{L}_1)$;

$$Y = \arccos\left\{\frac{\underline{S}'' \cdot \underline{L}}{|\underline{S}'' \times \underline{U}|}\right\} \quad , \quad \underline{L} \triangleq \underline{U} \times \underline{L}_1$$

$$Y = \arccos\left\{\frac{(\underline{S}')^T\, \underline{\underline{G}}\, \underline{L}}{|\underline{S}' \times \underline{\underline{G}}\, \underline{U}|}\right\}$$

where

$$\underline{N} \triangleq |\sin\zeta|\,\underline{L} + \cos\gamma\cos\zeta\,\underline{U} \tag{J-5}$$

It follows that, for $i = 1, 2, 3$,

$$\mathcal{H}_i = (-1/\sin^2\zeta\sin\gamma)(\underline{S}')^T(\partial\underline{G}/\partial X_i)\underline{N} \tag{J-6}$$

and γ is of course insensitive to X_4, X_5, and X_6. The row vectors $(\underline{S}')^T\partial\underline{G}/\partial X_i$ are determined from equations (H-9) to (H-10) using the conditions

$$(\underline{S}')^T\underline{G}_i = \underline{S}^T\underline{B}_i \tag{J-7}$$

and

$$(\underline{1}_3)^T(\underline{S}')\times\underline{G}_i = (\underline{K}')^T\underline{S}\times\underline{B}_i \tag{J-8}$$

in which each vector on the right was obtained by the transformation of its counterpart through the orthogonal matrix $\underline{B}_{m-1}$. With these relations substituted into the appropriate equations,

$$(\underline{S}')^T\partial\underline{G}/\partial X_1 = [0\ ,\ -\underline{S}^T\underline{B}_3\ ,\ \underline{S}^T\underline{B}_2] \tag{J-9}$$

$$(\underline{S}')^T\partial\underline{G}/\partial X_2 = [\cos X_1\,\underline{S}^T\underline{B}_3 - \sin X_1\,\underline{S}^T\underline{B}_2,\ \sin X_1\,\underline{S}^T\underline{B}_1\ ,\ -\cos X_1\,\underline{S}^T\underline{B}_1] \tag{J-10}$$

$$(\underline{S}')^T\partial\underline{G}/\partial X_3 = [(\underline{K}')^T\underline{S}\times\underline{B}_1\ ,\ (\underline{K}')^T\underline{S}\times\underline{B}_2\ ,\ (\underline{K}')^T\underline{S}\times\underline{B}_3] \tag{J-11}$$

and

$$\mathcal{H}_1 = (-1/\sin^2\zeta\sin\gamma)(-\underline{S}^T\underline{B}_3\eta_2 + \underline{S}^T\underline{B}_2\eta_3) \tag{J-12}$$

$$\mathcal{H}_2 = (-1/\sin^2\zeta\sin\gamma)[(\cos X_1\,\underline{S}^T\underline{B}_3 - \sin X_1\,\underline{S}^T\underline{B}_2)\eta_1 + \sin X_1\,\underline{S}^T\underline{B}_1\eta_2 - \cos X_1\,\underline{S}^T\underline{B}_1\eta_3] \tag{J-13}$$

$$\mathcal{H}_3 = (-1/\sin^2 \zeta \sin\gamma)\left[(\underline{K}' \cdot \underline{s} \times \underline{B}_1)\eta_1 + (\underline{K}' \cdot \underline{s} \times \underline{B}_2)\eta_2 + (\underline{K}' \cdot \underline{s} \times \underline{B}_3)\eta_3\right] \quad (J-14)$$

The preceding analysis was needed to determine accurate figures for measurement sensitivities. Instead of blindly applying these expressions in a complete simulation with an arbitrary measurement plan, however, it is highly desirable to further the investigation of these coefficients for whatever insight they will afford at the outset. It has already been demonstrated [J-1] that the magnitude and the direction of $(\mathcal{H}^T)$ can be used to precondition the incoming data, allowing predictions in regard to 1) the usefulness of various measurements, 2) the approximate "steady state" error for a given observation accuracy, and 3) the regions where nonlinearity problems can be anticipated. For this purpose the analysis is continued, with approximations introduced wherever necessary, in order to provide a final expression of such simplicity that the measurement geometry vector can be closely characterized immediately upon inspection.

First, it is noted that, for non-spinning satellites, the angular displacement traversed between measurements will be small. Therefore, the Euler angles will be small. For spinning satellites, the first two Euler angles (X_1, X_2) will be small if the spin axis is chosen along the vehicle z-axis.* Therefore $\underline{K}' \doteq \underline{B}_3$, and

*This does not in any way restrict the allowable direction of the spin axis relative to the orbit; in the simulation, any space orientation of the vehicle z-axis can be selected through specification of the initial C-matrix. Use of the z-axis does fix the spin along a principal inertia axis, but this is not a severe restriction. It should be noted that this procedure tends to minimize pitch rates, thus avoiding singularity. Finally, if the x-axis were used instead of the z-axis, this analysis is still qualitatively correct, as explained later in this section.

$$\underline{K}' \cdot \underline{S} \times \underline{B}_1 \doteq -\underline{S}^T \underline{B}_2 \qquad (J\text{-}15)$$

$$\underline{K}' \cdot \underline{S} \times \underline{B}_2 \doteq \underline{S}^T \underline{B}_1 \qquad (J\text{-}16)$$

$$\underline{K}' \cdot \underline{S} \times \underline{B}_3 \doteq 0 \qquad (J\text{-}17)$$

$$\sin X_1 \doteq 0 \; ; \quad \cos X_1 \doteq 1 \qquad (J\text{-}18)$$

and the approximate sensitivities are given by

$$\underline{\mathcal{H}}^T = (1/\sin^2 \zeta \sin Y)\, \underline{N} \times \underline{S}'' \qquad (J\text{-}19)$$

It is immediately evident that the sun sensor provides information primarily concerning the angular displacement about an axis normal to the plane defined by the sunline and the instrument vector $\underline{N}$. Recognition of this fact will be useful for the initial selection of measurement plans and for anticipating troublesome geometric configurations.*

As an aid in assessment of overall measurement sensitivity, the approximate magnitude of $\underline{\mathcal{H}}^T$ is $(1/\sin^2 \zeta \sin Y)\left[(\underline{N} \times \underline{S}'') \cdot (\underline{N} \times \underline{S}'')\right]^{1/2} =$

$$\frac{\left[(\underline{N} \cdot \underline{N})(\underline{S}'' \cdot \underline{S}'') - (\underline{N} \cdot \underline{S}'')^2\right]^{1/2}}{\sin^2 \zeta \sin Y} = \frac{\left\{\sin^2 \zeta + \cos^2 Y \cos^2 \zeta - \left[\sin S \underline{L} \cdot \underline{S}'' + \cos Y \cos S \underline{U} \cdot \underline{S}''\right]^2\right\}^{1/2}}{\sin^2 \zeta \sin Y}$$

*Consider a spin stabilized satellite with spin axis normal to the orbital plane which, in turn, is normal to the ecliptic. With one year, the situation will eventually arise in which all sun sensor measurements will be largely insensitive to the largest Euler angle of all.

$$= \frac{\left[\sin^2\zeta + \cos^2\gamma\cos^2\zeta - (\sin^2\zeta\cos\gamma + \cos^2\zeta\cos\gamma)^2\right]^{1/2}}{\sin^2\zeta\sin\gamma} = \frac{1}{|\sin\zeta|}$$

This leads to two important impliciations in regard to desired measurement geometry:

1) For a given value of (ζ), the sensitivity is essentially independent of (γ). Since values of γ near 0° or 180° are undesirable (because the plane of the angle and the algebraic sign of the deviation from nominal are ill defined) it follows that angles near 90° form the best measurements.

2) Angles formed with low values of (ζ) can be used to some advantage, but excessively high sensitivities could give rise to nonlinearity.

It remains to demonstrate that these two conclusions are valid when the vehicle spins about its roll axis (as in formulations in earlier Appendices), instead of the yaw axis. Briefly, the entire small angle analysis holds for spin angles of $2K\pi(K=1,2,3,\cdots)$; the sensitivities $\mathcal{H}_2$ and $\mathcal{H}_3$ are interchanged for spin angles of $(2K\pi + \pi/2)$; at intermediate spin angles a mere redistribution of sensitivity results.

APPENDIX K

MAGNETOMETER MEASUREMENTS AND SENSITIVITIES

A first approximation to the earth's magnetic field (which is adequate in this feasibility study) is a dipole with a magnetic moment $\underline{m}$, located at the earth center with a line of action at latitude 78.9° N and the earth longitude 70.1° W. The eastward celestial longitude at the equatorial intersection of the 70.1° W meridian is given in terms of an initial value ($\psi_{\beta 0}$) and the sidereal rate (ω_s) as illustrated in Fig. . This is used to determine the direction of $\underline{m}$ by the relation,

$$\underline{K}_\beta = \begin{bmatrix} k_{\beta 1} \\ k_{\beta 2} \\ k_{\beta 3} \end{bmatrix} = \begin{bmatrix} \cos 78.9^\circ \cos \psi_\beta \\ \cos 78.9^\circ \sin \psi_\beta \\ \sin 78.9^\circ \end{bmatrix} \tag{K-1}$$

The flux density $\underline{\beta}$ given in Fig. is easily reduced to

$$\underline{\beta} = (-\mu_\beta |\underline{m}|/4\pi)(\underline{K}_\beta \cdot \nabla)(\underline{R}/R^3) \tag{K-2}$$

which, in fixed inertial co-ordinates, has the components (n = 1,2,3):

$$\beta_n = (-\mu_\beta |\underline{m}|/4\pi)[k_{\beta n}/R^3 - 3(\underline{K}_\beta \cdot \underline{R})R_n/R^5] \tag{K-3}$$

The measured quantities are the components (β_n'') of the vector in body co-ordinates,

$$\underline{\beta}'' = \underline{\underline{B}}^T \underline{\beta} = \underline{\underline{G}}^T \underline{\underline{B}}_{m-1}^T \underline{\beta} = \underline{\underline{G}}^T \underline{\beta}' \tag{K-4}$$

$$\beta_n'' = \underline{G}_n^T \underline{\beta}' \tag{K-5}$$

the sensitivities are

$$\frac{\partial \beta_n''}{\partial X_i} = \left(\frac{\partial \underline{G}_n}{\partial X_i}\right)^T \underline{\beta}' \quad , i = 1,2,3 \tag{K-6}$$

MAGNETOMETER MEASUREMENT

CELESTIAL LONGITUDE OF MAG. POLE :

$$\psi_\beta = \psi_{\beta O} + \omega_S t$$

MAGNETIC POLE VECTOR :

$$\underline{K}_\beta \ (78.9°, \psi_\beta)$$

EARTH DIPOLE FIELD :

$$\underline{\beta} = \nabla \times \left\{ -(\mu_\beta / 4\pi) \left| \underline{m} \right| \underline{K}_\beta \times \nabla (1/r) \right\}$$

VEHICLE CO-ORDINATES:

$$\beta_n'' = \underline{B}_n^T \underline{\beta} = \underline{G}_n^T \underline{\beta}'$$

SENSITIVITY : $\partial \beta_n'' / \partial x_i = (\partial \underline{G}_n / \partial x_i)^T \underline{\beta}'$

APPROXIMATE SENSITIVITY : CROSS PRODUCT OF

$\underline{\beta}$ WITH (n^{TH}) VEHICLE AXIS

where the vector partial derivatives $(\partial \underline{G}_\eta / \partial X_i)$ are again taken directly from equations (K-9) to (K-11) and the vector $\underline{\beta}'$ is an independently known quantity.

Again using the small angle approximations in the partial derivatives $(\partial \underline{G} / \partial X_i)$ it is seen that

$$\eta = 1 : \underline{\mathcal{H}} \doteq [0, \underline{G}_3^T \underline{\beta}', -\underline{G}_2^T \underline{\beta}'] = [0 \quad \beta_3'' \quad -\beta_2''] \tag{K-7}$$

$$\eta = 2 : \underline{\mathcal{H}} \doteq [-\beta_3'' \quad 0 \quad \beta_1''] \tag{K-8}$$

$$\eta = 3 : \underline{\mathcal{H}} \doteq [\beta_2'' \quad -\beta_1'' \quad 0] \tag{K-9}$$

Equation K-6 provides accurate values for measurement sensitivities, whereas (K-7) to (K-9) can be used for data conditioning criteria. Since $\underline{\mathcal{H}}_\eta^T$ is near the cross product of $\underline{\beta}$ with the (η^{th}) vehicle axis, three considerations are immediately apparent:

1) A magnetometer with its sensitive axis instantaneously parallel to $\underline{\beta}$ will provide no attitude information.

2) The sensitivities experience their greatest changes at lower values of the angle between $\underline{\mathcal{H}}^T$ and $\underline{\beta}$. Readings of magnetometers in these positions should be avoided to prevent nonlinearity errors.

3) A magnetometer will be most effective when its sensitive axis is situated such that $\underline{\mathcal{H}}^T$ is close to the principal eigenvector of the attitude uncertainty covariance matrix. [K-1]

As in the preceding section, the use of a roll spin axis formulation will not invalidate the conclusions regarding data conditioning.

REFERENCES FOR APPENDIX

A-1. Danby, J.M.A., Fundamentals of Celestial Mechanics, New York, MacMillan, 1962, p.7.

A-2. Ibid., pp. 155-166.

A-3. Stuelpnagel, J., "On the Parametrization of the Three-Dimensional Rotation Group," SIAM Rev. 6, 422 (1964).

B-1. Nidey, R.A., "Gravitational Torque on a Satellite of Arbitrary Shape", ARSJ 30, 203-204 (1960).

B-2. Roberson, R.E., "Gravitational Torque on a Satellite Vehicle," J. Franklin Inst. 265, 13-22 (1958).

B-3. Polyakhova, Ye.N., "Solar Radiation Pressure and the Motion of Earth Satellites," AIAAJ 1, 2893 (1963).

B-4. Goldstein, H., Classical Mechanics, Addison-Wesley, Reading, Mass., 1959, p. 158.

D-1. Ibid., pp. 159 - 163.

D-2. Thompson, W.T., Introduction to Space Dynamics, New York, Wiley, 1963, pp. 113-118.

E-1. Clancy, T.F., and T.P. Mitchell, "Effects of Radiation Forces on the Attitude of an Artificial Earth Satellite," AIAAJ 2,517-524 (1964).

E-2. Beletskii, V.V., "Motion of an Artificial Earth Satellite About its Center of Mass", Artificial Earth Satellites, edited by L. V. Kurnosova (Plenum Press, Inc., New York, 1960) vol. 1, p 49.

F-1. DeBra, D.B. and R.H. Delp, "Rigid Body Attitude Stability and Natural Frequencies in a Circular Orbit," J. Astronaut. Sci. 8, 14-17 (1961).

F-2. Kane, T.R., "Attitude Stability of Earth-Pointing Satellites", AIAAJ 3, 726-731 (1965).

F-3. Auelmann, R.R., "Regions of Libration for a Symmetrical Satellite," AIAA J 1,1445-1447 (1963).

F-4. Pringle, R., "Bounds on the Librations of a Symmetrical Satellite", AIAA J 2,908 (1964).

I-1. Kalman, R.E., "A New Approach to Linear Filtering and Prediction Problems", Trans ASME Series D (J. Basic Eng.) 82,35-45 (1960).

I-2. Schlegel, L.B., "Covariance Matrix Approximation", AIAA J 1,2672-2673 (1963).

I-3. Hitzl, D.L., "Comments on 'Covariance Matrix Approximation'," AIAA J3, 1977-1978 (1965).

J-1. Farrell, J., "Simulation of a Minimum Variance Orbital Navigation System", AIAA J Spacecraft and Rockets 3, 91-98 (1966).

K-1. Battin, R.H., "A Statistical Optimizing Navigation Procedure for Space Flight", ARSJ 32, 1681-1696 (1962).